0026-895X/03/6404-848–856$7.00
MOLECULAR PHARMACOLOGY
Vol. 64, No. 4
2628/1093216
Mol Pharmacol 64:848–856, 2003
Printed in U.S.A.

Mutations in the Epithelial Na^+ Channel ENaC Outer Pore Disrupt Amiloride Block by Increasing Its Dissociation Rate

STEPHAN KELLENBERGER, IVAN GAUTSCHI, and LAURENT SCHILD

Institut de Pharmacologie et de Toxicologie, Université de Lausanne, Lausanne, Switzerland

Received April 30, 2003; accepted June 24, 2003

This article is available online at http://molpharm.aspetjournals.org

ABSTRACT

The epithelial Na^+ channel ENaC mediates transepithelial Na^+ transport in the distal kidney, the colon, and the lung and is a key element for the maintenance of Na^+ balance and the regulation of blood pressure. Mutagenesis studies have identified residues αS583 and the homologous βG525 and γG537 in the outer pore entrance that are critical for ENaC block by the K^+-sparing diuretic amiloride. The aim of the present study was to determine first, whether these residues are part of the amiloride binding site, and second, whether they are general determinants of ENaC block by amiloride and its derivatives. Kinetic analysis of the association and dissociation rates of amiloride and benzamil to ENaC showed that mutation of residue αS583C and the homologous βG525C increased the dissociation rate of the drugs from the binding site, with little changes in their association rate. Thus, these mutations destabilize the binding interaction between the blockers and the receptor on the channel, favoring the unbinding of the ligand. This strongly suggests that they are part of the binding site. Because mutations of αS583, βG525, and γG537 have similar effects on amiloride, benzamil, and triamterene block, we conclude that these three ENaC blockers share a common receptor within the ion channel pore.

The highly selective epithelial Na^+ channel ENaC belongs to a new class of proteins called the ENaC/degenerin (DEG) superfamily, which includes a variety of proteins found in mammals, nematodes, flies, and snails that are involved in transepithelial Na^+ transport, mechanotransduction, and neurotransmission (Mano and Driscoll, 1999; Kellenberger and Schild, 2002). ENaC expressed in the apical membrane of epithelial cells mediates sodium reabsorption in the distal nephron, the colon, and the lung. In the distal nephron, ENaC activity is tightly regulated by aldosterone and vasopressin, serving to fine-tune renal Na^+ excretion (Garty and Palmer, 1997). This fine regulation of the distal sodium handling is critical for the maintenance of a balance between sodium intake and elimination. Genetic defects of ENaC activity lead either to severe hypertension in case of channel gain-of-function as found in Liddle syndrome or to salt losing nephropathy in case of loss of ENaC function in pseudohypoaldosteronism type-1 (Hansson et al., 1995; Chang et al., 1996; Lifton et al., 2001).

Sodium absorption in the distal nephron is tightly linked to potassium excretion. Pharmacological blockers of ENaC such as amiloride or triamterene increase renal Na^+ excretion and decrease K^+ excretion and are therefore used as K^+-sparing diuretics. Amiloride and its derivative benzamil are high-affinity blockers of ENaC from the external side with an IC_{50} in the submicromolar range (Kleyman and Cragoe, 1988; Garty and Palmer, 1997). Initial work on amiloride block of the epithelial Na^+ channel showed that amiloride interacts competitively with the permeant Na^+ or Li^+ ions, suggesting that amiloride binds within the external vestibule of the channel pore acting as a channel pore blocker (Palmer and Andersen, 1989; Palmer, 1990).

ENaC is formed by homologous subunits that have two membrane-spanning segments (M1 and M2) linked by a large extracellular loop. ENaC is a heterotetramer made of 2α, 1β, and 1γ subunits arranged pseudosymmetrically around the channel pore in a $\alpha\beta\alpha\gamma$ configuration. Structure-function experiments showed that mutations of amino acid residues in the extracellular loop close to M2 of α, β, and γ ENaC subunits dramatically decrease the channel affinity for amiloride (Schild et al., 1997). These amino acid residues, αS583, and the homologous βG525 and γG537 are accessible from the extracellular side and are located directly upstream of the selectivity filter, indicating that they represent a potential binding site for amiloride in the external channel pore.

However, direct evidence that the residues αS583, βG525, and γG537 indeed form the amiloride binding site is still lacking. It remains possible that these mutations induce steric changes that indirectly affect amiloride block by impairing the accessibility of the ligand to its binding site. In

This work was supported by grant 3100-059217.99 from the Swiss National Foundation for Scientific Research (to L.S.). S.K. was supported by a National Institutes of Health Specialized Center for Research in Atherosclerosis grant for hypertension.

ABBREVIATIONS: ENaC, epithelial Na^+ channel; DEG, degenerin; M2, second transmembrane domain; P_o, open probability; wt, wild type.

addition, it is still unknown whether amiloride analogs and triamterene share with amiloride the same receptor.

To answer these questions, we have investigated the effects of mutations of αS583, βG525, and γG537 on amiloride, benzamil, and triamterene block of ENaC current at the macroscopic and at the single-channel level. We show that these mutations equally affect ENaC block by the three agents tested, indicating that these drugs share a common blocking mechanism. We provide evidence that the mutations lower the affinity of the channel to amiloride and benzamil by increasing the dissociation rate of the blocker from its receptor. We conclude that αS583, βG525, and γG537 are part of the receptor for ENaC blockers in the external channel pore.

Materials and Methods

Site-Directed Mutagenesis and Expression in *Xenopus laevis* Oocytes. Site-directed mutagenesis was performed on rat ENaC cDNA as described previously (Schild et al., 1997). Complementary RNAs of each αβγ subunit were synthesized in vitro. Stage V-VI oocytes were surgically removed from the ovarian tissue of female *X. laevis* frogs that had been anesthetized by immersion in MS-222 (2 g/l; Sandoz, Basel, Switzerland). The oocytes were defolliculated, and healthy stage V and VI *X. laevis* oocytes were pressure-injected with 100 nl of a solution containing equal amounts of α, β, and γ ENaC subunits or α and β subunits at a total concentration of 100 ng/μl. To obtain a lower channel density for αβγ ENaC single-channel patches we reduced the amount of RNA injected. For simplicity, mutants are named by the mutated subunit only, although always all three subunits (α, β and γ) were coexpressed, where not noted explicitly.

Electrophysiological Analysis. Electrophysiological measurements were taken at 16 to 48 h after injection. Macroscopic currents for drug inhibition curves were recorded using the two-electrode voltage-clamp technique at a holding potential of −100 mV. Currents were recorded with a TEV-200 amplifier (Dagan, Minneapolis, MN) equipped with two bath electrodes. For drug inhibition curves, the solution contained 70 mM *N*-methyl D-glucamine, 20 mM NaCl, 20 mM KCl, 10 mM HEPES, and 0.2 mM $CaCl_2$, pH 7.4. An analogous solution, in which the 20 mM NaCl was replaced by 20 mM *N*-methyl D-glucamine, was used to determine the zero current level. Amiloride, benzamil, and triamterene were from Sigma (Buchs, Switzerland) and all other chemicals were from Sigma or Fluka (Buchs, Switzerland).

Single-channel currents and macroscopic currents for the determination of the blocker off-rate were measured in the outside-out configuration of the patch-clamp technique essentially as described previously (Kellenberger et al., 1999b). The external solution in patch-clamp experiments contained 110 mM NaCl or LiCl, 1.8 mM $CaCl_2$, and 10 mM HEPES-NaOH, pH 7.35. The Na^+ concentration of this solution was different from that of solutions used for whole-cell current measurements. Because Na^+ is known to compete with amiloride for its binding site (Garty and Palmer, 1997), we have measured amiloride block of wt ENaC at different Na^+ concentrations with the two-electrode voltage-clamp to quantify the effect of Na^+. The IC_{50} of amiloride block was 0.07 ± 0.01 μM (n = 145) in Na^+-free extracellular solution containing 20 mM Li^+ as conducting ion, 0.11 ± 0.01 μM (n = 24) with 20 mM extracellular Na^+, and 0.24 ± 0.01 μM (n = 17) with 110 mM extracellular Na^+. This shows that the effect of Na^+ concentration on amiloride block is relatively small in our experimental conditions. Changing of extracellular solutions in patch-clamp experiments was done using the Rapid Solution Changer RSC-200 (Biologic, Claix, France). The pipette solution contained 75 mM CsF, 17 mM *N*-methyl-D-glucamine, 10 mM EGTA, and 10 mM HEPES, pH 7.35. The inclusion of fluoride facilitated the formation of stable excised outside-out patches.

Pipettes were pulled from Borosilicate glass (WPI, Sarasota, FL). Pipettes for macropatches were used with a resistance of 1 to 3 MΩ, and pipettes for single-channel measurements had a resistance of 4 to 10 MΩ, when filled with the pipette solution. In patch-clamp experiments, currents were recorded with a List EPC-9 patch clamp amplifier using a PC-based data acquisition system (Pulse; HEKA Electronic, Lambrecht/Pfalz, Germany) and filtered at 1,000 to 2,000 Hz for single-channel analysis. Single-channel openings were detected by standard half-amplitude threshold analysis using TAC 4.09 (Bruxton Corporation, Seattle, WA). Patches for the kinetic analysis of αβ ENaC channels contained one single channel. Other patches contained one to four channels. Channel number was estimated from the maximum number of overlapping openings. Open times and closed times were analyzed from the binned data with durations >200 μs, using TACFIT (Bruxton Corporation). In channels with short closings (as the mutants αS583C and βG525C in the presence of amiloride or benzamil), open duration time constants may be overestimated because of missed short closings. This error was in all cases less than 4%, as calculated according to Colquhoun and Hawkes (1995).

It is known that ENaC channels can be found with very different open probabilities (P_o). Experiments were performed on αβγ ENaC channels with $P_o \geq 0.2$, which constituted the majority of the ENaC in our patches. In addition, changes in P_o during the course of the experiment may affect the result. In our conditions of excised outside-out patch-clamp recording, ENaC activity in some experiments slightly decreased during the first 2 to 3 min after formation of the excised patch. Then, it generally stabilized at a new level. To reduce errors caused by a possible slow rundown of channel activity, we alternated the different experimental conditions (i.e., absence of drug, presence of drug at different concentrations) several times during the lifetime of the patch. The following analysis of P_o in experiments with αβ ENaC illustrates the stability of channel activity over time. The P_o of unblocked channels was 0.93 ± 0.06 at the beginning and 0.95 ± 0.02 at the end of the experiments. Averaged data are presented as mean ± S.E.M.

Results

A Common Binding Site for Amiloride and Its Analogs. Individual substitutions by cysteine of the residues αS583, βG525, and γG537, located in the external pore entry of ENaC, shift the concentration for half-maximal inhibition (IC_{50}) to a ~20-fold higher concentration for the mutation in the α subunit, and to a ~1,000-fold higher concentration for the β and γ mutations (Schild et al., 1997) (see alignment Fig. 1A). To determine whether these mutations have the same effect on other blockers of ENaC, we have tested the current inhibition by the amiloride-derivative benzamil and the analog triamterene (Fig. 1B). In ENaC wt, the IC_{50} for benzamil block is 11 nM and the IC_{50} for triamterene block is 4.5 μM (Fig. 1C). Thus, compared with amiloride, which has an IC_{50} of ~0.1 to 0.2 μM (Garty and Palmer, 1997; Schild et al., 1997), ~10-fold lower concentrations of benzamil, and ~50-fold higher concentrations of triamterene are needed to block ENaC. The 10-fold higher affinity for benzamil relative to amiloride is probably caused by an additional hydrophobic interaction as a result of the added benzyl group. It should also be noted that only the protonated form of amiloride blocks ENaC (Garty and Palmer, 1997). The pK_a of triamterene is 6.2, compared with 8.7 for amiloride. Thus, at pH 7.4, 95% of amiloride, but only 6% of triamteren is protonated, explaining in part the different concentration dependence of ENaC block. The mutations in the α, β, and γ subunit (αS583, βG525, and γG537) shifted the IC_{50} values

for benzamil to 5-, 1180-, and 320-fold higher concentrations (Fig. 1C). The triamterene IC_{50} was shifted by a factor of 5 by the αS583C mutation. Triamterene at a concentration of 1 mM inhibited only ~20% of currents carried by ENaC containing the mutations βG525C and γG537C. Because of the limited solubility of triamterene, it was not possible to test higher concentrations. Thus, it was not possible to determine exactly the IC_{50} of triamterene block of ENaC containing the β or γ mutation; however, the data suggest that the mutations shift the inhibition curve of triamterene by a similar extent to higher concentrations as observed with amiloride and benzamil inhibition (Fig. 1C). These data show that αS583, βG525, and γG537 mutations affect similarly the block of ENaC by amiloride, benzamil, and triamterene, suggesting overlapping binding sites for these ligands.

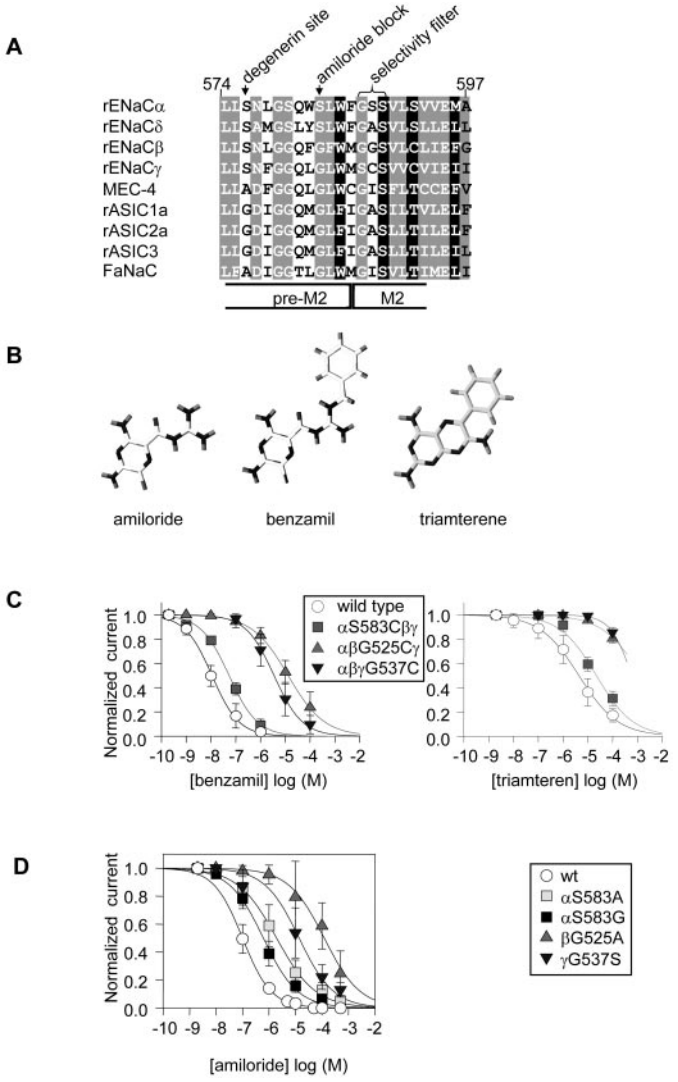

Fig. 1. Inhibition of αβγ ENaC by amiloride and analogs. A, alignment of the ENaC pore region. The pre-M2 segment and the NH_2-terminal part of M2 are shown, which make up the outer pore entry and selectivity filter of ENaC. The location of the degeneration-inducing mutation, the residues critical for amiloride block, and the selectivity filter are indicated on top. Numbering indicates the rat α-ENaC amino acid position. Black shading indicates 100% conserved and gray shading indicates 80% or greater conserved. B, chemical structure of the three drugs used. C, inhibition curve of Na^+ current by benzamil (left) and triamterene (right) from oocytes expressing wt or mutant αβγ ENaC. The Na^+ current was measured in individual oocytes in the presence of different concentrations of the drugs, using the two-electrode voltage-clamp technique at −100 mV. IC_{50} values from fits were for benzamil block, wt, 0.011 ± 0.002 μM; αS583, 0.054 ± 0.006 μM; βG525C, 13.0 ± 0.5 μM; and γS537C, 3.5 ± 0.4 μM; and for triamterene block, wt, 4.5 ± 0.5 μM; αS583, 23.9 ± 4.3 μM; βG525C, 1450 ± 181 μM; and γS537C, 601 ± 8 μM. C, amiloride block of conservative mutations was determined as described above. IC_{50} values from fits are for wt, 0.10 ± 0.01 μM; αS583A, 1.93 ± 0.22 μM; αS583G, 0.61 ± 0.07 μM; βG525A, 122 ± 19 μM; and γG537S, 13.7 ± 0.8 μM. n = 5 to 13.

We have verified the importance of the αS583, βG525, and γG537 residues on ENaC block by amiloride, by generating more conservative amino acid substitutions than cysteine substitutions, i.e., mutations of Ser (αENaC) to Ala and Gly, and of Gly (β, γ) to Ser and/or Ala. As shown in Fig. 1D, the mutations αS583G and αS583A shifted the IC_{50} of amiloride block by a factor of 6 and 19, respectively; the mutation βG525A by a factor of 1,220; and the mutation γG537S by a factor of 136. This indicates that mutations to Ala cause the same shift of the inhibition curves as mutations to Cys, whereas mutations to Ser or Gly have a smaller, but significant effect on channel block by amiloride.

Kinetics of αβENaC Block. The ENaC block by amiloride or analogs corresponds to a reversible binding process according to a simple model as follows:

$$C \underset{\beta}{\overset{\alpha}{\rightleftarrows}} O + \text{Ligand} \underset{k_{off}}{\overset{k_{on}(\text{Ligand})}{\rightleftharpoons}} B \times \text{Ligand} \qquad (1)$$

where α and β are the opening and closing rate constants of the channel, respectively, and k_{on} and k_{off} are the association and dissociation rate constants, respectively, for the ligand L (e.g., amiloride). This model implies that binding of the ligand to a single site of the open channel, O, results in a blocked state B of the channel complexed with the ligand L. We assume that the blocker binds to the open channel, although no experimental evidence excludes the possibility that amiloride can also bind to the closed channel C. Simulation with this and a more complex model involving a blocked state of the closed channel showed that both models gave essentially the same result (data not shown). The scheme predicts that the dwell times of the open state, τ_o, and the dwell times of the blocked state of the channel, τ_B, are inversely proportional to k_{on} and k_{off} according to the following relationships:

$$\tau_O^{-1} = k_{on}[\text{Ligand}] + \beta \qquad (2)$$

and

$$\tau_B^{-1} = k_{off} \qquad (3)$$

These relationships indicate that the time constant for the blocked state of the channel τ_B is independent of the amiloride concentration. It should be pointed out that according to eq. 2, the time constant for the open state depends not only on the k_{on} for amiloride but also on the rate constant of the channel closing, β.

To determine the association rate of the blocker, we analyzed single-channel recordings of ENaC activity obtained from excised outside-out patches. We first used ENaC formed by α and β subunits only, which are almost equally sensitive to inhibition by amiloride or by benzamil compared with αβγ ENaC (Fig. 2A). The advantage of using αβ ENaC is that this channel is almost constantly open; therefore, blocking events can be readily distinguished from the fast channel closings

(McNicholas and Canessa, 1997; Fyfe and Canessa, 1998). Figure 2B shows single-channel traces of $\alpha\beta$ EnaC, illustrating that channel closings are rare and extremely short (uppermost trace in Fig. 2B). Addition of benzamil to the extracellular solution induced transitions to the zero current level of longer duration than the short closures, indicating that they represent benzamil-induced blocking events. The dwell time of the channel open state shortens with increasing concentration of benzamil, as predicted by eq. 2, and depends at high drug concentrations essentially on the drug association rate constant k_{on}. This is shown qualitatively by the representative current traces in Fig. 2B and quantitatively in Fig. 2C, where the reciprocal of the open state lifetime is plotted against the benzamil concentration. The k_{on} for benzamil can be calculated according to eq. 2 and corresponds to the slope of $1/\tau_{open}$ in Fig. 2C as $57 \pm 3\ \mu M^{-1}s^{-1}$. The corresponding value for the amiloride k_{on} was $68 \pm 15\ \mu M^{-1}s^{-1}$ (Table 1), indicating that the association rate of both ligands to the receptor on $\alpha\beta$ ENaC is basically the same.

As shown in eq. 3, the dissociation rate constant for amiloride/benzamil corresponds to the reciprocal of the channel blocked-state lifetime. According to eq. 1, the nonconducting states of the channel represent either closed channels or channels blocked by the drug.

The closed time histogram in the absence of benzamil shows a main component with a time constant of 4 ms (Fig. 3A). In the presence of 10 nM benzamil, longer nonconducting states occur (Fig. 3B) that are clearly different from the short closed states of the channel and therefore represent blocking events. The closed time histogram shows the presence of this new component of closed times that represents the blocking events with a time constant τ_B of 244 ± 82 ms. As mentioned previously, the time constant τ_B corresponds to the average residency time of benzamil on its binding site in the channel pore. The reciprocal of τ_B corresponds to the benzamil k_{off} (eq. 3) and is independent of the benzamil concentration as shown in Fig. 3C. The equilibrium dissociation rate constant can be calculated from the microscopic k_{off} and k_{on} values:

$$K_D = k_{off}/k_{on} \quad (4)$$

The value obtained matches very well the inhibitory constant IC_{50} determined from current inhibition curves in Fig. 2A

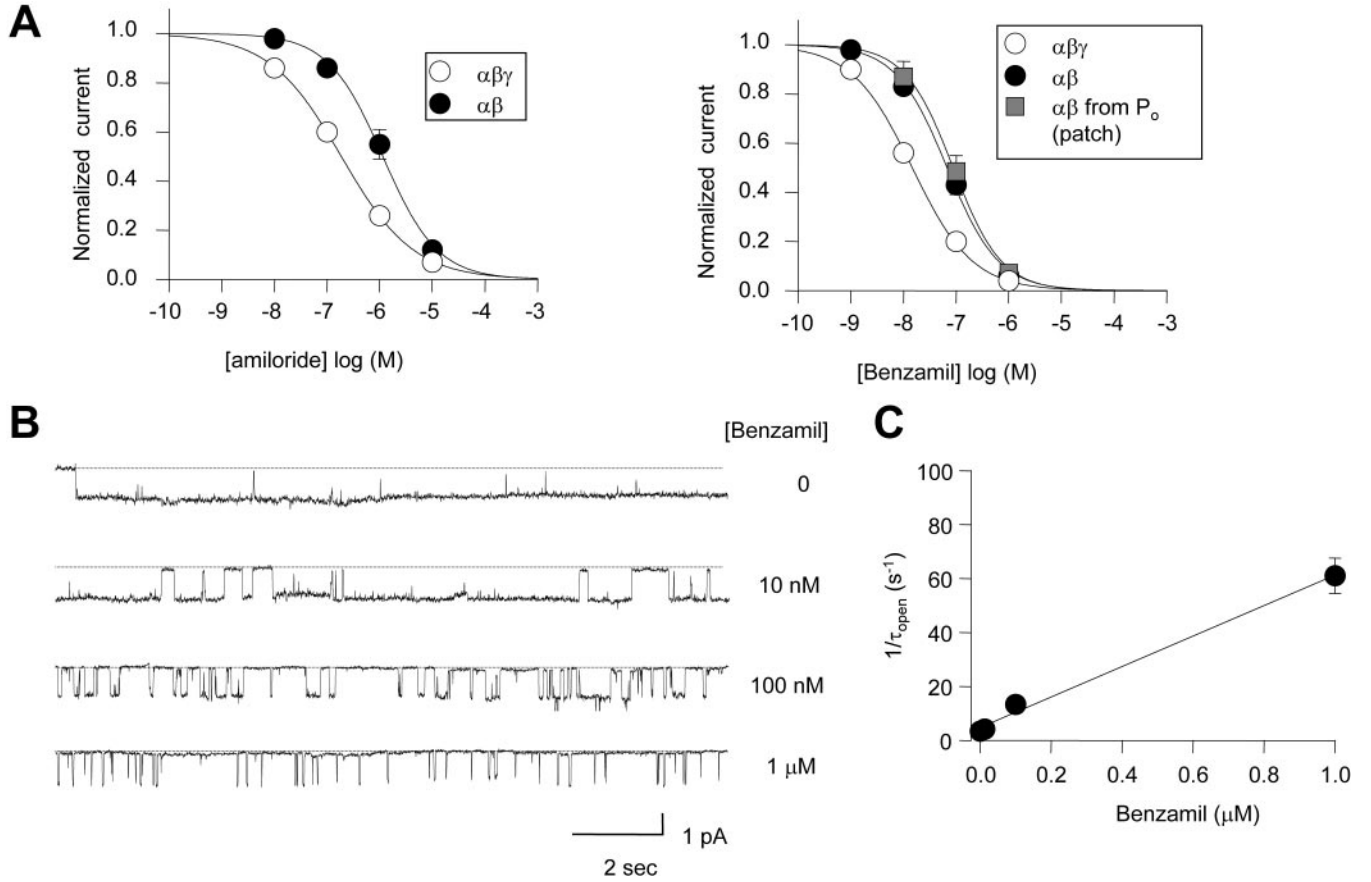

Fig. 2. Benzamil block of $\alpha\beta$ ENaC. A, inhibition curve of Na^+ current by amiloride (left) and benzamil (right) from oocytes expressing $\alpha\beta$ ENaC. The experiments were done as described in the legend to Fig. 1C. For benzamil, an inhibition curve was in addition constructed from the dependence of channel open probability P_o on benzamil concentration ($n = 2$ patches). IC_{50} values from fits were for amiloride block, $\alpha\beta\gamma$ ENaC, $0.19 \pm 0.00\ \mu M$, $\alpha\beta$ ENaC $1.15 \pm 0.01\ \mu M$, for benzamil block $\alpha\beta\gamma$ ENaC, $0.015 \pm 0.001\ \mu M$, $\alpha\beta$ ENaC $0.068 \pm 0.005\ \mu M$, $\alpha\beta$ ENaC, from P_o, $0.088 \pm 0.007\ \mu M$. B, representative current traces from an outside-out patch containing a single active $\alpha\beta$ ENaC channel. The holding potential was -100 mV, channel activity was recorded in the presence of increasing concentrations of benzamil in the extracellular solution, as indicated in the figure. The baseline (nonconductive state) is indicated by the dotted line. C, dependence of channel open times on benzamil concentration. The reciprocal of channel open times determined as described under *Materials and Methods* in the presence of different benzamil concentrations is plotted versus the benzamil concentration. The solid line represents the linear regression to the data with slope $= 56.6 \pm 2.9\ s^{-1}$ and constant $= 4.8 \pm 1.5\ s^{-1}$, which represent according to eq. 2 the association rate k_{on} and the closing rate β.

(both 0.07 μM). To further confirm that ENaC block is the same in whole oocytes and in excised patches, we have determined benzamil block in single-channel patches by plotting the channel open probability P_o versus the benzamil concentration (Fig. 2A, right). Both approaches yielded the same concentration dependence for benzamil block.

TABLE 1

Open dwell times and drug association rates k_{on}

Open times were measured in the presence of a high concentration of the drug. The on-rate k_{on} was calculated from eq. 2 at a drug concentration of 1 μM. Data were obtained from n = 1 to 4 different patches and several hundred to >1,000 events per condition.

Mutant	Amiloride		Benzamil	
	Open Dwell Time	k_{on}	Open Dwell Time	k_{on}
	ms	$\mu M^{-1}s^{-1}$	*ms*	$\mu M^{-1}s^{-1}$
wt ($\alpha\beta\gamma$)	12 ± 1	80 ± 8	14 ± 2	68 ± 6
αS583C	9.1	107	N.D.	N.D.
βG525C	37 ± 11	22 ± 7	46 ± 3	17 ± 1
$\alpha\beta$	14 ± 3	68 ± 15	16 ± 2	57 ± 3

N.D., not determined.

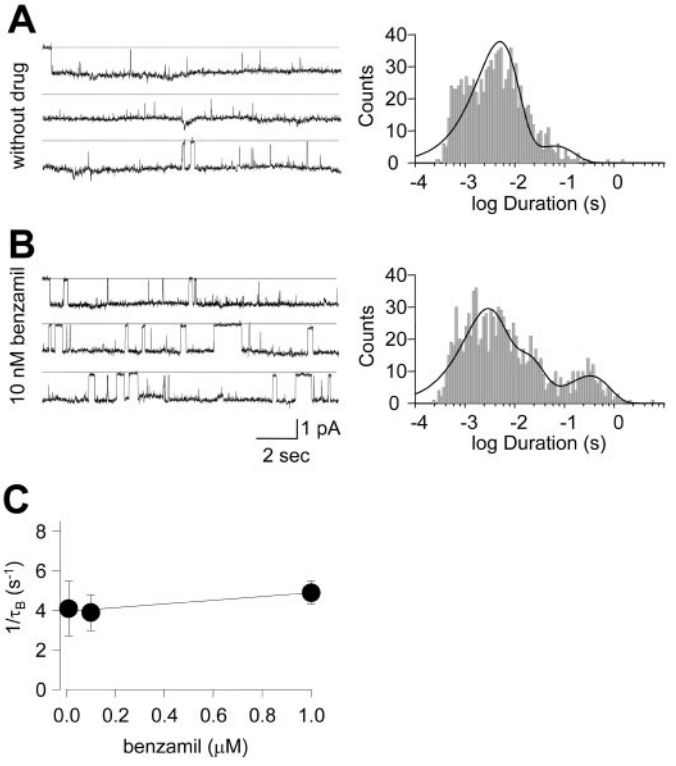

Fig. 3. Determination of the benzamil dissociation rate k_{off} from single-channel currents of $\alpha\beta$ ENaC. A, channel activity in the absence of the blocker. Left, representative current traces from an outside-out patch containing a single active $\alpha\beta$ ENaC channel at a holding potential of −100 mV. Right, representative closed time distribution of $\alpha\beta$ ENaC in the absence of benzamil. The distribution was fitted with one major component of τ_{c1} = 4.9 ms (relative weight, 0.88) and a small component τ_{c2} = 64.0 ms (relative weight, 0.12). B, channel activity in the presence of 10 nM benzamil. Left, representative current traces and the right, the distribution of nonconductive states. The distribution was fitted with two components for the closed times, τ_{c1} = 2.4 ms (0.51) and τ_{c2} = 14.7 ms (0.31) and one component for channel block, τ_B = 329 ms (w = 0.18). Mean values for τ_{c1} and τ_B from two patches containing one single active $\alpha\beta$ channel each were 4.1 ± 0.8 and 244 ± 82 ms, respectively. C, plot of $1/\tau_B$ measured at different benzamil concentrations versus benzamil concentration, data from two to three single-channel patches per condition. The solid line represents the linear regression to the data with slope = 1.04 ± 0.45 s^{-1} and constant = 3.81 ± 0.27s^{-1}. The constant ($1/\tau_B$) represents according to eq. 3 the dissociation rate k_{off}.

Block of wt and Mutant $\alpha\beta\gamma$ ENaC. The gating of $\alpha\beta\gamma$ ENaC typically consists of spontaneous transitions between long open and closed states as illustrated by the traces in Fig. 4A. Typical open state and closed state dwell times are of the order of hundreds of milliseconds to seconds (Garty and Palmer, 1997; Kellenberger et al., 2002). This slow gating mode complicates the kinetic analysis of the ENaC block by amiloride and benzamil because blocking events by amiloride are of about the same dwell time duration as channel closed states. In Fig. 4A, a single-channel trace of $\alpha\beta\gamma$ ENaC in the presence of 1 μM amiloride shows short channel openings separated by transitions to nonconducting states, which could be either closings or blocking events by amiloride. Thus, according to eq. 1 the rate constants for channel opening (β) and for amiloride dissociation (k_{off}) cannot be distinguished and therefore not precisely determined.

Equation 2 predicts that in the presence of amiloride, the reciprocal of the open-state lifetime should be linearly related to the concentration of the blocker as already shown for benzamil block of $\alpha\beta$ ENaC (Fig. 2B). This is confirmed for amiloride block of $\alpha\beta\gamma$ ENaC in Fig. 4B, which plots the relationship between the reciprocal of the open-state lifetime and the amiloride concentration. The k_{on} values for amiloride and benzamil determined from such experiments are 80 ± 8 and 68 ± 8 $\mu M^{-1}s^{-1}$ (Table 1) and are not significantly different from the values obtained in the $\alpha\beta$ ENaC channel. These experiments confirm that the higher affinity of benzamil relative to amiloride for ENaC is not caused by differences in their respective k_{on}. The measured association rate for amiloride to $\alpha\beta\gamma$ ENaC is similar to that estimated from noise analysis of cloned $\alpha\beta\gamma$ ENaC (80 $\mu M^{-1}s^{-1}$; Segal et al., 2002) and higher than the association rate estimated by the same technique for block of Na^+ current in frog skin (13 $\mu M^{-1}s^{-1}$; Li et al., 1985).

We then asked whether the lower affinity of the αS583C and βG525C ENaC mutants to amiloride and benzamil (Fig. 1) could have been caused by a lower association rate constant of the blockers to their receptor. The αS583C$\beta\gamma$ ENaC in the presence of 1 μM amiloride shows bursts of short openings and closings separated by longer closed times (Fig. 4A). For comparison, the wt $\alpha\beta\gamma$ ENaC shows similar short openings in the presence of 1 μM amiloride (compare Fig. 4A and Table 1); however, the closed/blocked dwell times are shorter in the αS583C mutant. The $\alpha\beta$G525Cγ mutant in the presence of 1 μM benzamil displays open times that are substantially longer than those of ENaC wt with 1 μM benzamil, indicating that this mutation slows the blocker on-rate to some extent. With 10 μM benzamil, however, the open times are further reduced (Fig. 4A). The quantitative analysis of channel open times (Table 1) shows that the drug on-rate is slightly increased in ENaC containing the mutation αS583C with regard to ENaC wt, whereas it is ~4 times decreased in βG525C mutant channels. The determination of the amiloride and/or benzamil association rates with low-affinity ENaC mutants indicates that the small changes in the blocker on-rate that we observe cannot account for the 30- to 1,000-fold decrease in the mutant channel affinity for the blocker.

As mentioned previously, the determination of the appar-

ent dissociation rate constants of amiloride and benzamil from single channel analysis of ENaC wt are problematic because channel blocking events are undistinguishable from channel closures. However, for the ENaC mutants the duration of the nonconducting states induced by amiloride or benzamil; i.e., the nonconductive states within bursts (compare traces obtained in the presence/absence of the blocker) are much shorter than in the wt ENaC (Fig. 4A). This suggests that the mutations αS583C and βG525C may increase the dissociation of the blocker from its receptor site, probably by destabilizing the binding interaction between the ligand and the receptor. We measured the duration of the nonconductive states within bursts of single channels in the αS583Cβγ and αβG525Cγ mutants. The analysis of the dwell time distribution of these nonconductive states yielded time constants of 26 ms for amiloride block of αS583Cβγ and 27 ± 2 ms for benzamil block of αβG525Cγ ENaC, corresponding to k_{off} values of 38 and 37 s^{-1}, respectively. Thus, these values are clearly increased over the k_{off} of benzamil from αβ ENaC (4 ± 1.4 s^{-1}; Fig. 3B).

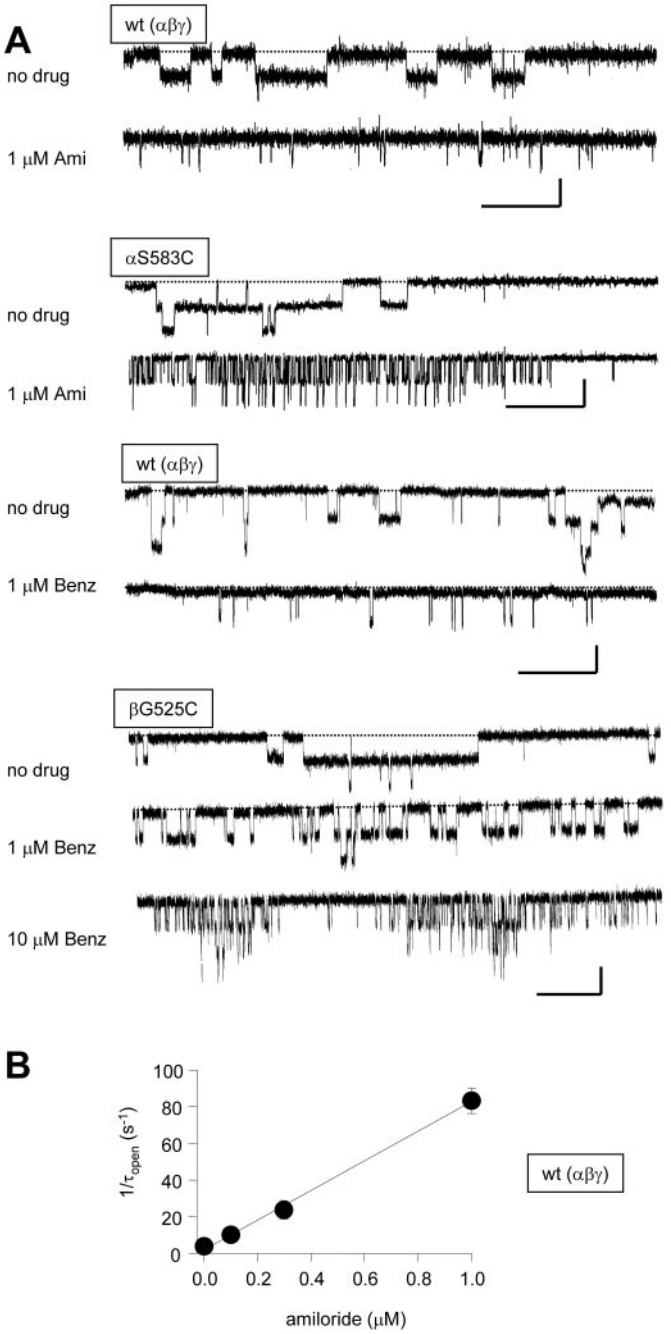

Fig. 4. Single-channel currents of wt and mutant αβγ ENaC in the absence and presence of channel blockers. A, representative single-channel current traces obtained from outside-out patches at −100 mV in Na^+ Ringer solution from patches containing one to four active channels. Traces are from αβγ wt ENaC or the mutants αS583C and βG525C in the absence or the presence of amiloride or benzamil, as indicated in the figure. The bars correspond to 1 s and 0.5 pA. B, dependence of wt ENaC channel open times on amiloride concentration. The reciprocal of channel open times determined as described under *Materials and Methods* in the presence of different amiloride concentrations is plotted versus the amiloride concentration. The solid line represents the linear regression to the data with slope = 80.6 ± 2.7 s^{-1} and constant = 2.0 ± 1.4 s^{-1}, which represent according to eq. 2 the association rate k_{on} and the closing rate β.

To directly compare the mutants with the wt ENaC in αβγ channels, we used in addition an alternative approach to determine the dissociation rate of amiloride and benzamil from ENaC, which consisted in measuring the time course of Li^+ current recovery after rapid removal of the ENaC blocker. Excised outside-out macropatches were obtained from oocytes expressing ENaC wt or mutants, and placed in the solution stream of a rapid solution exchanger device. This setting allowed a rapid and complete washout of benzamil or amiloride in the external solution. The speed of the perfusion change was monitored for each experiment by measuring the appearance of an inward current after the rapid substitution of the external nonconducting K^+ ion by conducting Li^+ ions. On average, this yielded a time constant of 17 ± 4 ms for the exchange of the external solution. Current traces in macropatches of αβγ ENaC wt and mutant, generated by the rapid washout of amiloride or benzamil from the bath are shown in Fig. 5. With wt ENaC macropatches, the appearance of the inward Li^+ current after washout of amiloride follows a single exponential, and the rate of appearance determined by the best fit of the tracing gave a value of 2.1 ± 0.4 s^{-1} ($\tau \cong$ 0.5 s; Table 2). The rate of current appearance corresponds to the dissociation of bound amiloride, and this dissociation rate is close to the dissociation rates estimated by noise analysis from cloned ENaC and from Na^+ current in frog skin, which were 9 and 4 s^{-1} (Li et al., 1985; Segal et al., 2002). The rate of appearance of the Li^+ current after rapid removal of external benzamil was slower with a rate constant of 0.11 ± 0.03 s^{-1}. This is consistent with the lower dissociation rate constant for benzamil compared with amiloride that we have measured from single channel activity of αβ ENaC. This lower dissociation rate can account for the higher affinity for ENaC of benzamil relative to amiloride. The recovery of the inward Li^+ current after amiloride washout was extremely fast in αS583Cβγ and αβG525Cγ ENaC mutants compared with the wt. Under these conditions, the speed of the fluid exchange becomes limiting for the determination of the rate constant of current recovery. Therefore, we have analyzed in the ENaC mutants the time course of Li^+ current recovery from benzamil inhibition because of its slower time course compared with amiloride. Figure 5 clearly shows that in the αS583Cβγ and αβG525Cγ mutants the current recovery from benzamil inhibition was much faster than for the wild type. In Fig. 5, the insets displaying the recording in a 10-fold expanded time scale show that current recovery is faster for αβG525Cγ than for αS583Cβγ. The dissociation rate con-

stants k_{off} obtained from this analysis are comparable with those determined from single-channel kinetics. They are 20- and 200-fold increased in the mutants αS583C$\beta\gamma$ and $\alpha\beta$G525Cγ relative to ENaC wt (Table 2).

We can conclude from these experiments that the increase in the dissociation rate can account for most of the differences in benzamil affinity between the ENaC wt and the ENaC αS583C$\beta\gamma$ and $\alpha\beta$G525C mutants. The k_{off} of αS583C$\beta\gamma$ ENaC is increased by a factor of 10 and 24 for amiloride and benzamil, respectively, explaining the 10- to 20-fold shift in macroscopic inhibition curves. The βG525C mutation induces a 187-fold increase in k_{off} and a 4-fold decrease in the k_{on} for benzamil. The resulting calculated 750-fold shift in IC_{50} is close to the ~1,000-fold shift observed.

Discussion

We have investigated the effects of ENaC αS583, βG525, and γG537 mutations on the kinetics of channel block by amiloride and benzamil. These two high-affinity blockers differ in their affinity to ENaC. We show here that this is because of their different dissociation rates from the receptor in the ENaC pore. Mutations of αS583, βG525, and γG537 decrease the affinity of ENaC for amiloride and benzamil essentially by increasing the dissociation rate of the ligands, with little changes in their association rate to the receptor. In other words, these mutations destabilize the binding interaction between the blockers and the receptor on the channel, favoring the unbinding of the ligand. These effects on the

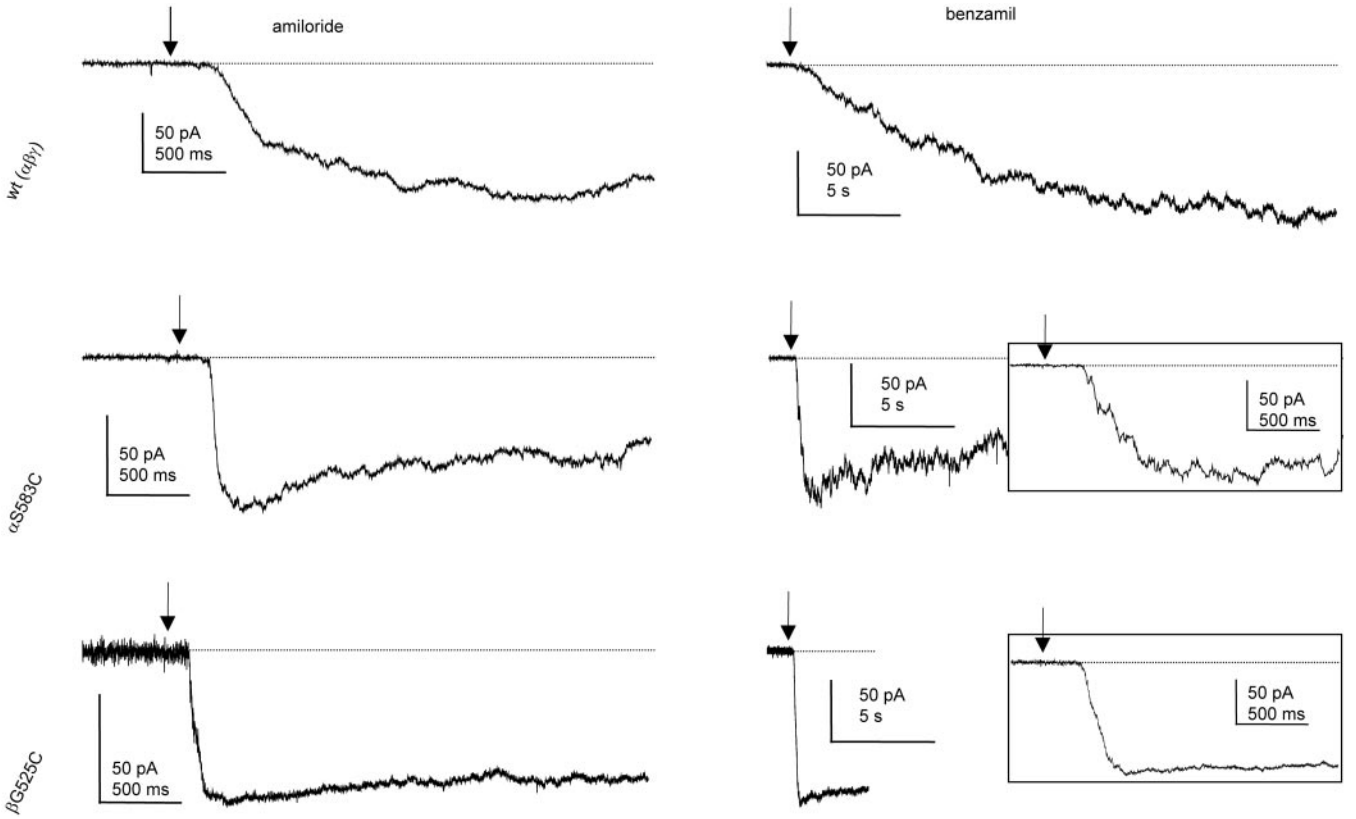

Fig. 5. Dissociation of amiloride and benzamil from wt and mutant ENaC. Washout of amiloride and benzamil from ENaC wt and the αS583C and βG525C mutant channels was measured in excised outside-out macropatches at −100 mV. Channel currents were blocked by external perfusion of a high concentration of the blocker. At the time indicated by the arrow, this solution was rapidly replaced by a blocker-free solution. The speed of the solution change was determined by changing from a K^+ solution to a Li^+ solution (see text). The current recovery represents the dissociation of the channel blocker. Note the different time scales for amiloride and benzamil experiments. Insets on the right show the time course of current recovery at an expanded time scale. Exponential fits to these and similar experiments yielded time constants of current increase that were used to calculate dissociation rate constants k_{off} according to eq. 3 and that are shown in Table 2.

TABLE 2

Dissociation rates k_{off} and calculated K_D values

Macroscopic currents were recorded from outside-out macropatches at −100 mV. The solution was switched from one containing amiloride or benzamil at a high concentration (1–100 μM) to a solution without drug. The resulting current increase was fitted to a single exponential τ and the off-rate k_{off} was calculated as $1/\tau$. n = 2 to 4 experiments per condition. The equilibrium dissociation constant K_D was calculated from on- and off-rates taken from Tables 1 and 2 as indicated.

	k_{off}		$K_D = k_{off}/k_{on}$	
Mutant	Amiloride	Benzamil	Amiloride	Benzamil
	s^{-1}		μM	
wt($\alpha\beta\gamma$)	2.09 ± 0.40	0.11 ± 0.03	0.026 ± 0.008	0.002 ± 0.001
αS583C	27.6 ± 2.96	2.66 ± 0.65	0.258 ± 0.028	N.D.
βG525C	N.D.	20.6 ± 5.9	N.D.	1.212 ± 0.071
$\alpha\beta$	17.0 ± 3.0	3.19 ± 0.73	0.250 ± 0.099	0.054 ± 0.020

N.D., not determined.

ligand-receptor interactions indicate that residues αS583, βG525, and γG537 are part of the receptor for amiloride and benzamil located in the external entry of the channel pore. Because mutations of αS583, βG525, and γG537 have similar effects on amiloride, benzamil, and triamterene block, we conclude that these three ENaC blockers share a common receptor.

The Amiloride Binding Site. Early experiments on frog skin showed that amiloride block is voltage-dependent, suggesting that the binding site on ENaC is within the transmembrane electrical field. These experiments also provided evidence for an interaction between extracellular Na^+ and amiloride block (Palmer and Andersen, 1989; Garty and Palmer, 1997). Based on these observations, it was suggested that amiloride may block the channel by a simple physical occlusion of the pore.

This study together with other recent molecular studies places the amiloride binding site in the extracellular pore region. First, residues αS583, βG525, and γG537 are located only four amino acid residues away, in the N-terminal direction, from the selectivity filter sequence G/SxS in the ion permeation pathway (Kellenberger et al., 1999a,b). Second, evidence that residues αS583, βG525, and γG537 are extracellular comes from the observation that substitution by cysteine and subsequent modification by hydrophilic sulfhydryl reagents results in channel block (Schild et al., 1997; Kosari et al., 1998; Snyder et al., 1999). The αS583C mutant is blocked by Zn^{2+} with an affinity in the micromolar range (Firsov et al., 1998). This high-affinity block requires the αS583C mutations on the two αENaC subunits of the heteromultimeric channel. If the αENaC subunits face each other across the channel pore as suggested by a study using concatameric constructs (Firsov et al., 1998), this would imply that the optimal distance for coordinated ligation of Zn^{2+} of ~5 Å (Krovetz et al., 1997) would correspond to the distance between the two αS583 residues across the pore.

The observation that substituting cysteine residues at the amiloride binding site can form a high-affinity Zn^{2+} binding site and that they can be modified by sulfhydryl reagents indicates that their side chains are oriented toward the lumen of the pore entry. Our finding that very conservative mutations of these residues affect amiloride block further supports this conclusion.

After the identification of the critical role of the homologous αS583, βG525, and γG537 in amiloride binding, additional mutations were made in this region of the protein in the search of other residues that contribute to the amiloride binding site. In the α subunit, the mutation αW582L increased the IC_{50} by a factor of ~30 (Schild et al., 1997). Several mutations in the pore region were shown to increase the IC_{50} by 2- to 4-fold (Sheng et al., 2000). Other mutations may affect indirectly channel block by amiloride. Mutation of αS588 to Iso but not Ala shifted the IC_{50} to ~20-fold higher concentrations, and some mutations of βG529 also reduced the sensitivity to amiloride block (Waldmann et al., 1995b; Kellenberger et al., 1999b). Thus, residues near αS583 and βG525 probably participate directly or indirectly in amiloride block but to a much lesser extent than αS583, βG525, and γG537.

Amiloride Block in Other ENaC/DEG Family Members. The amino acid sequence constituting the amiloride binding site is highly conserved among the members of the ENaC/degenerin channel family. However, ENaC/degenerin channels differ in their respective sensitivity to block by amiloride, with ENaC having the highest affinity. Interestingly, ENaC differs from the other channels of this family by a Ser residue at position αS583, whereas other ENaC/degenerin channels such as acid-sensing ion channels and degenerins carry a Gly residue. This Ser-Gly-Ser-Gly arrangement is unique for ENaC and might in part account for its high affinity for amiloride because the αS583G mutation decreases its affinity (Fig. 1D). However, the heteromeric and functional δβγ ENaC that also carries a Ser residue at the position homologous to α583 in the δ subunits, has a lower affinity for amiloride than αβγ ENaC (Waldmann et al., 1995a). Inversely, degenerin channels formed by MEC-4 and MEC-10, which both have a glycine at the homologous position, display an IC_{50} for amiloride of 0.4 μM, thus very close to that of ENaC (Goodman et al., 2002). Differences between ENaC/DEG channels in the sequence near the amiloride binding site may account for their different pharmacological profile. For example, *X. laevis* εβγ ENaC shows a 10-fold higher IC_{50} than *X. laevis* αβγ ENaC because of a Leu-to-Trp substitution at the position corresponding to residue 584 in *rat* αENaC (Babini et al., 2003). Interaction between amiloride and ENaC for high-affinity block is complex and may involve other, still unidentified residues in the extracellular loop of ENaC/DEG channels.

Structure-activity studies of different amiloride analogs on wild-type and mutant ENaC will certainly refine our understanding of the binding interactions between blockers and the amiloride receptor. This will provide the basis for the future understanding of the structure of the amiloride binding site and the external pore of ENaC. We hope that such studies will help the design and the identification of molecules able to block other members of the ENaC/DEG channel family such as acid-sensing ion channels for which high-affinity blockers are still needed.

Acknowledgments

We thank J. D. Horisberger for reading of a previous version of the manuscript.

References

Babini E, Geisler H-S, Siba M, and Grunder S (2003) A new subunit of the epithelial Na^+ channel identifies regions involved in Na^+ self-inhibition. *J Biol Chem* **278:** 28418–28426.

Chang S, Grunder S, Hanukoglu A, Rosler A, Mathew P, Hanukoglu I, Schild L, Lu Y, Shimkets R, Nelson-Williams C, et al. (1996) Mutations in subunits of the epithelial sodium channel cause salt wasting with hyperkalaemic acidosis, pseudohypoaldosteronism type 1. *Nat Genet* **12:**248–253.

Colquhoun D and Hawkes AG (1995) The principles of the stochastic interpretation of ion-channel mechanisms, in *Single-Channel Recording*, 2nd ed (Sakmann B and Neher E eds) pp 453–457, Plenum Press, New York.

Firsov D, Gautschi I, Merillat AM, Rossier BC, and Schild L (1998) The heterotetrameric architecture of the epithelial sodium channel (ENaC). *EMBO (Eur Mol Biol Organ) J* **17:**344–352.

Fyfe GK and Canessa CM (1998) Subunit composition determines the single channel kinetics of the epithelial sodium channel. *J Gen Physiol* **112:**423–432.

Garty H and Palmer LG (1997) Epithelial sodium channels - function, structure and regulation. *Physiol Rev* **77:**359–396.

Goodman MB, Ernstrom GG, Chelur DS, O'Hagan R, Yao CA, and Chalfie M (2002) MEC-2 regulates *C. elegans* DEG/ENaC channels needed for mechanosensation. *Nature (Lond)* **415:**1039–1042.

Hansson JH, Schild L, Lu Y, Wilson TA, Gautschi I, Shimkets R, Nelson-Williams C, Rossier BC, and Lifton RP (1995) A *de novo* missense mutation of the β subunit of the epithelial sodium channel causes hypertension and Liddle syndrome, identifying a proline-rich segment critical for regulation of channel activity. *Proc Natl Acad Sci USA* **92:**11495–11499.

Kellenberger S, Gautschi I, and Schild L (1999a) A single point mutation in the pore region of the epithelial Na^+ channel changes ion selectivity by modifying molecular sieving. *Proc Natl Acad Sci USA* **96:**4170–4175.

Kellenberger S, Gautschi I, and Schild L (2002) An external site controls closing of the epithelial Na^+ channel ENaC. *J Physiol (Lond)* **543.2:**413–424.

Kellenberger S, Hoffmann-Pochon N, Gautschi I, Schneeberger E, and Schild L (1999b) On the molecular basis of ion permeation in the epithelial Na^+ channel. *J Gen Physiol* **114:**13–30.

Kellenberger S and Schild L (2002) Epithelial sodium channel/degenerin family of ion channels: a variety of functions for a shared structure. *Physiol Rev* **82:**735–767.

Kleyman TR and Cragoe EJ Jr (1988) Amiloride and its analogs as tools in the study of ion transport. *J Membr Biol* **105:**1–21.

Kosari F, Sheng SH, Li JQ, Mak DD, Foskett JK, and Kleyman TR (1998) Subunit stoichiometry of the epithelial sodium channel. *J Biol Chem* **273:**13469–13474.

Krovetz HS, VanDongen HMA, and VanDongen AMJ (1997) Atomic distance estimates from disulfides and high-affinity metal-binding sites in a K^+ channel pore. *Biophys J* **72:**117–126.

Li JH, Cragoe EJ Jr, and Lindemann B (1985) Structure-activity relationship of amiloride analogs as blockers of epithelial Na channels: I. Pyrazine-ring modifications. *J Membr Biol* **83:**45–56.

Lifton RP, Gharavi AG, and Geller DS (2001) Molecular mechanisms of human hypertension. *Cell* **104:**545–556.

Mano I and Driscoll M (1999) DEG/ENaC channels: a touchy superfamily that watches its salt. *Bioessays* **21:**568–578.

McNicholas CM and Canessa CM (1997) Diversity of channels generated by different combinations of epithelial sodium channel subunits. *J Gen Physiol* **109:**681–692.

Palmer LG (1990) Epithelial Na channels: the nature of the conducting pore. *Renal Physiol Biochem* **13:**51–58.

Palmer LG and Andersen OS (1989) Interactions of amiloride and small monovalent cations with the epithelial sodium channel. Inferences about the nature of the channel pore. *Biophys J* **55:**779–787.

Schild L, Schneeberger E, Gautschi I, and Firsov D (1997) Identification of amino acid residues in the α, β, γ subunits of the epithelial sodium channel (ENaC) involved in amiloride block and ion permeation. *J Gen Physiol* **109:**15–26.

Segal A, Awayda MS, Eggermont J, Van Driessche W, and Weber WM (2002) Influence of voltage and extracellular Na^+ on amiloride block and transport kinetics of rat epithelial Na^+ channel expressed in *Xenopus* oocytes. *Pfluegers Arch Eur J Physiol* **443:**882–891.

Sheng SH, Li JQ, McNulty KA, Avery D, and Kleyman TR (2000) Characterization of the selectivity filter of the epithelial sodium channel. *J Biol Chem* **275:**8572–8581.

Snyder PM, Olson DR, and Bucher DB (1999) A pore segment in DEG/ENaC Na^+ channels. *J Biol Chem* **274:**28484–28490.

Waldmann R, Champigny G, Bassilana F, Voilley N, and Lazdunski M (1995a) Molecular cloning and functional expression of a novel amiloride-sensitive Na^+ channel. *J Biol Chem* **270:**27411–27414.

Waldmann R, Champigny G, and Lazdunski M (1995b) Functional degenerin-containing chimeras identify residues essential for amiloride-sensitive Na^+ channel function. *J Biol Chem* **270:**11735–11737.

Address correspondence to: Dr. Stephan Kellenberger, Institut de Pharmacologie et de Toxicologie, Bugnon 27, Université de Lausanne CH-1005, Lausanne Suisse, Switzerland. E-mail: stephan.kellenberger@ipharm.unil.ch